

## Varying Relative Degradation Rates of Oil in Different Forms and Environments Revealed by Ramped Pyrolysis

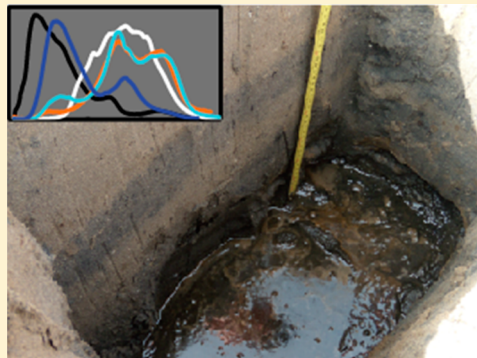
Matthew A. Pendergraft<sup>§,†</sup> and Brad E. Rosenheim<sup>\*,†</sup>

<sup>§</sup>Department of Earth and Environmental Sciences, Tulane University, New Orleans, Louisiana 70118, United States

<sup>†</sup>College of Marine Science, University of South Florida, Saint Petersburg, Florida 33701, United States

### Supporting Information

**ABSTRACT:** Degradation of oil contamination yields stabilized products by removing and transforming reactive and volatile compounds. In contaminated coastal environments, the processes of degradation are influenced by shoreline energy, which increases the surface area of the oil as well as exchange between oil, water, sediments, microbes, oxygen, and nutrients. Here, a ramped pyrolysis carbon isotope technique is employed to investigate thermochemical and isotopic changes in organic material from coastal environments contaminated with oil from the 2010 BP Deepwater Horizon oil spill. Oiled beach sediment, tar ball, and marsh samples were collected from a barrier island and a brackish marsh in southeast Louisiana over a period of 881 days. Stable carbon (<sup>13</sup>C) and radiocarbon (<sup>14</sup>C) isotopic data demonstrate a predominance of oil-derived carbon in the organic material. Ramped pyrolysis profiles indicate that the organic material was transformed into more stable forms. Our data indicate relative rates of stabilization in the following order, from fastest to slowest: high energy beach sediments > low energy beach sediments > marsh > tar balls. Oil was transformed most rapidly where shoreline energy and the rates of oil dispersion and exchange with water, sediments, microbes, oxygen, and nutrients were greatest. Still, isotope data reveal persistence of oil.



### 1. INTRODUCTION

When oil contaminates an environment, multiple processes physically disperse the oil and chemically transform it in a process referred to as weathering. The processes that chemically change the oil, as well as their effects, can be collectively referred to as oil degradation, and include evaporation, biodegradation, dissolution/water washing, photo-oxidation/photodegradation, emulsification, and adsorption/sedimentation.<sup>1–12</sup> These degradative processes remove and/or convert reactive and volatile compounds and leave behind stabilized residues that can persist in the environment.<sup>4,5,11–13</sup>

Oil degradation rates are determined by various factors,<sup>4,5,9,14,15</sup> with shoreline energy being one of the most important for coastal oil spills.<sup>1,9</sup> Microbes can consume upward of 50% of spilled oil<sup>4</sup> and biodegradation rates are largely influenced by coastline energy.<sup>1,5,9</sup> Greater shoreline energy (wind, waves, and tides) increases biodegradation rates by accelerating oil dispersion, which increases oil surface area available to microbes<sup>16–18</sup> and the supply of oxygen and nutrients (N and P) necessary for microbes to consume oil.<sup>19–21</sup> High shoreline energy has been shown to correspond to high rates of weathering,<sup>1,9</sup> and longer oil persistence has been observed on protected coastlines.<sup>22</sup> Perhaps the longest-studied oil spill, the 1969 *Florida* spill in West Falmouth, Massachusetts, resulted in oil persisting in a protected saltmarsh with low shoreline energy for three decades.<sup>23–25</sup> White et al.<sup>25</sup> concluded that physical processes ultimately decide the fate of residual oil components at West Falmouth.

The large extent of the 2010 BP Deepwater Horizon oil spill (DwH) provides an opportunity to study degradation and transformation of oil deposited synchronously in different coastal environments. DwH is the largest accidental oil spill to date, having released roughly 10 times the volume of oil as the 1989 *Exxon Valdez* oil spill in the Gulf of Alaska.<sup>26</sup> Approximately 1600 km of Gulf of Mexico shoreline and 75 linear km of Louisiana coastal marsh received moderate to heavy oiling from DwH.<sup>27,28</sup> Coastal Louisiana is comprised of multiple environments including barrier islands directly exposed to the energy of the Gulf of Mexico and semiprotected marshes that receive a diminished, yet substantial, portion of that energy. The wetlands of this region constitute about 37% of the coastal wetlands of the 48 conterminous United States,<sup>29,30</sup> support roughly 30% of the total United States fishing industry, and protect a network of infrastructure responsible for an equal proportion of the country's oil and gas supply.<sup>30</sup> At the same time, the Mississippi River Delta suffers from significant subsidence-driven land loss estimated at 4877 km<sup>2</sup> during 1932 to 2010,<sup>29</sup> and expected to reach 10 000+ km<sup>2</sup> by the year 2100.<sup>31</sup> Oil contamination can negatively impact marshes<sup>30,32</sup> and accelerated marsh shoreline erosion due to DwH has been documented.<sup>33</sup> Assessment of

Received: April 7, 2014

Revised: June 28, 2014

Accepted: August 8, 2014

Published: August 8, 2014



the degradation of oil in this ecosystem through time is important to discern where and how oil degradation products may contribute to further stress on the coastal wetlands.

Here we employ ramped pyrolysis (RP) carbon isotope analysis<sup>34</sup> to oil-impacted organic material from a barrier island and a brackish marsh in order to test the hypothesis that oil will be removed from the coastal environment before postdepositional oil transformation occurs. The RP isotope technique analyzes all acid insoluble organic material (OM) in a sample and produces both a pyrolysis profile related to thermochemical stability and an isotopic spectrum (<sup>14</sup>C and <sup>13</sup>C) resulting from the different components of admixed OM.<sup>34–38</sup> The RP isotope technique has been previously shown to be effective at detecting and quantifying oil contamination in sedimentary organic material (SOM)<sup>39</sup> as it employs radiocarbon analysis, a sensitive tracer of oil-derived organic carbon (OC). Effectively, oil and residual compounds from its degradation lie on the completely radiocarbon-depleted endmember of the radiocarbon scale ( $\Delta^{14}\text{C} = -1000\text{\textperthousand}$ )<sup>40</sup> and recent sediments and soils OC lies on the other end (near or slightly above 0‰), with analytical precision on radiocarbon measurements generally around 5–10‰. The use of <sup>14</sup>C for oil spill studies<sup>25,41–46</sup> is not as prevalent as the use of <sup>13</sup>C,<sup>47–57</sup> mainly because of the relatively high cost and the novelty of these measurements compared to stable isotope analyses. Ultimately, this approach applied to these environments can provide a basis for ongoing remediation efforts and efforts to assess the toxicity of oil contamination and its degradation derivatives.

## 2. MATERIALS AND METHODS

**2.1. Sample Locations.** Grand Isle and Bay Jimmy in southeast Louisiana were sampled over the course of 881 days following the Macondo well blow-out that initiated DwH (Figure 1). Grand Isle is a subtropical barrier island at the mouth of Barataria Bay with a gently sloping sandy beach affected by moderate wave energy, which increases episodically during tropical cyclones (summer) and cold fronts (winter). Two locations at Grand Isle were repeatedly sampled for sediments and tar balls: a relatively high energy site exposed to direct wave energy from the Gulf of Mexico and a relatively low energy site located on the lagoonal side of Grand Isle, protected from direct wave action from the Gulf of Mexico. The third sampling location was at Bay Jimmy, which lies within the brackish marsh region of northeastern Barataria Bay.<sup>58</sup> Although an erosive marsh with ~10s of km of southerly fetch, the Bay Jimmy site is considered a lower energy environment compared to the two barrier island sites, which have even greater southerly fetch. During the course of our sampling, we observed more geomorphic change at the Grand Isle sites than at the Bay Jimmy site.

**2.2. Sample Collection and Treatment.** Sediments and tar balls were collected from Grand Isle and oiled marsh plants and sediments were collected from Bay Jimmy. At Grand Isle, sediment was initially sampled from the beach surface, then, after geomorphic changes mixed the oil deposits into the beach sediments, by digging trenches (~1 m depth) near the shoreline and sampling dark subsurface layers and oily sheen with a petrochemical odor at the trench bottoms (see abstract figure for an annotated photograph of a representative trench). Tar balls on the beach between the two fixed sites and an oil/tar coating on a rocky groin near the higher energy site were also collected from Grand Isle. We use the general term of “tar

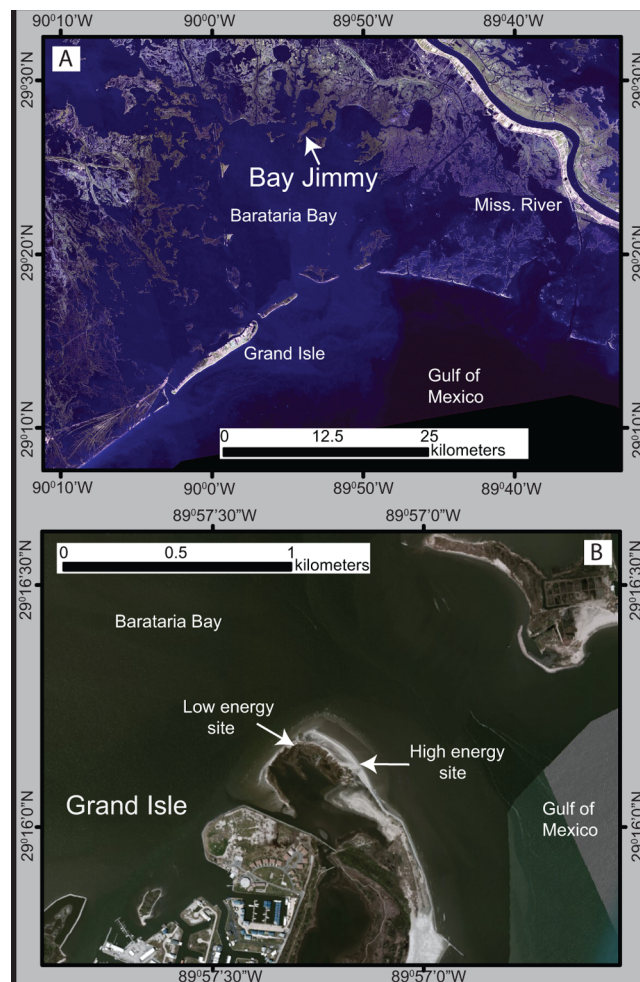


Figure 1. Sampling locations in Bay Jimmy (A.) and at Grand Isle (B.) in southeast Louisiana. Sample locations shown by arrows.

balls” for a nonuniform set of samples with varying proportions of oil/tar and sediments collected from the surface. Marsh samples from Bay Jimmy include clusters of oil and vegetation and the top (0–1 cm) of a 50 cm surface core collected with a hand auger.

Most samples were collected in glassware capped with aluminum foil (both precombusted at 525 °C for ≥2 h) and a plastic lid, and stored at –4 °C under nitrogen gas. Some samples from Bay Jimmy were collected in sealed plastic bags (Whirlpack/Ziploc) when precombusted glassware was exhausted, but the samples were transferred to precombusted glass once in the laboratory (~3 h after sampling). The crude oil, provided by BP (reference material ID: SOB-20100617-032; source sample ID: ENT-052210-OL-041/043), was sampled directly from the Macondo wellhead and stored at –4 °C.

Samples from Grand Isle were ground with a mortar and pestle, acidified with 10% hydrochloric acid (HCl) to remove inorganic carbon, then repeatedly rinsed with deionized water, centrifuged, decanted until a pH of ~6 was reached, and then dried at 60 °C for 24 h or until completely dry. Acidification of samples was necessary to analyze the organic material without inclusion of thermal decomposition of carbonate-carbon. It has been demonstrated that rinsing sediments and soils containing organic material after acid treatment can mobilize some of the organic matter,<sup>59</sup> however the resulting ambiguity of pyrolyzing

samples containing carbonate minerals was considered a higher cost to our experimental approach. Thus, samples from Bay Jimmy were also acid treated after inspection for and removal of shell fragments, to ensure that all samples were treated equally for this experiment.

**2.3. Elemental and Stable Isotope Analyses.** Samples were measured for organic carbon content (%OC) and bulk stable carbon isotopic composition ( $\delta^{13}\text{C}$ ), then subjected to ramped pyrolysis carbon isotope analysis. Organic carbon content and stable carbon signatures were measured on 127 beach sediment, tar ball, and marsh samples (Figure S1, Supporting Information (SI)) at the Stable Isotope Laboratory at Tulane University using an Elementar vario MICRO cube elemental analyzer interfaced to an Isoprime dual inlet isotope ratio mass spectrometer (EA-IRMS) continuously monitoring isotope ratios of  $\text{CO}_2$  peaks in the carrier gas of He. Values of % OC were used to calculate sample size and expected yields for RP analysis in order to evaluate for complete carbon recovery. Stable carbon isotopic signatures are expressed in  $\delta$  notation and ‰ units, relative to the Pee Dee Belemnite (PDB) standard.<sup>60</sup>

**2.4. Ramped Pyrolysis  $^{14}\text{C}$  Analysis.** Sixty of the 127 samples were screened for reaction profiles using RP. Based on this screening, 15 representative samples were reanalyzed by RP with  $\text{CO}_2$  collection and isotopic analysis of the  $\text{CO}_2$ . The same RP procedure was used as in previous studies;<sup>34–39</sup> this procedure consists of a smooth temperature ramp of 5 °C min<sup>-1</sup>, 0% O<sub>2</sub> in the reaction chamber, and ~8% O<sub>2</sub> in the combustion chamber. More details of the analysis can be found in Rosenheim et al.<sup>34</sup> Individual pyrolysis peaks, representing thermochemically distinct components, were cryogenically collected at inflection points in continuous aliquots.

Radiocarbon and stable carbon isotope analyses of the ramped pyrolysis  $\text{CO}_2$  aliquots were conducted at the National Ocean Sciences Accelerator Mass Spectrometer facility (NOSAMS) at Woods Hole Oceanographic Institution. Radiocarbon data, reported in  $\Delta$  notation and per mil (‰) units, were calculated using

$$\Delta^{14}\text{C} \cong \delta^{14}\text{C} = (F_m - 1) \times 1000 \quad (1)$$

where  $F_m$  is the fraction of the  $^{14}\text{C}/^{12}\text{C}$  ratio of the measured sample compared to that of a “modern” standard (1950 wood).<sup>40</sup> We assume  $\Delta^{14}\text{C}$  to be equivalent to  $\delta^{14}\text{C}$  because less than three years passed between sample collection and measurement.<sup>40</sup> Ramped pyrolysis AMS radiocarbon data are corrected for an analytical blank (9.3 ± 9.3 µg modern blank and 0.5 ± 0.5 µg  $^{14}\text{C}$ -free blank for an entire run; these masses are divided by the number of isotopic measurements made during each run) determined by repeated measurements on isotope standards. Nine RP aliquots were depleted enough in  $^{14}\text{C}$  that they resulted in less  $^{14}\text{C}$  than our determination of blank contamination in the method. These values are treated as they were in Pendergraft et al.;<sup>39</sup> we use a minimum  $\Delta^{14}\text{C}$  limit equivalent to  $2\sigma$  uncertainty of the blank to report fraction modern values and to calculate  $\Delta^{14}\text{C}$  values.

### 3. RESULTS

Depleted radiocarbon values ( $-891 \pm 232\text{‰}$ ; Figure 2 and SI Table S2) dominate the aliquots of  $\text{CO}_2$  collected during RP, with the exception of the marsh surface sample collected at 678 d, which had no visible oil. Stable carbon isotopic signatures ( $-27.5 \pm 2.2\text{‰}$ ; Figure 2 and SI Table S2) are also generally

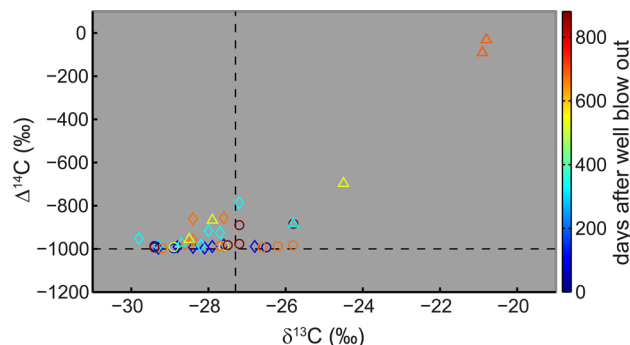


**Figure 2.** Radiocarbon ( $\Delta^{14}\text{C}$ ) and stable carbon ( $\delta^{13}\text{C}$ ) data for the  $\text{CO}_2$  aliquots produced and collected during RP display a dominance of oil in the OC for this sample set, with the exception of the aliquots from the marsh sample from 678 d. Dashed lines are at the isotopic signatures of the Macondo oil. Symbols indicate sample type: diamond—beach SOM; triangle—marsh SOM; circle—tar ball. Colors represent sampling date and are scaled to the color bar.

depleted relative to Gulf of Mexico marine SOC ( $-21.4 \pm 1.9\text{‰}$ ).<sup>38</sup> We calculate a geometric mean isotopic value (equivalent to a bulk isotopic value) using

$$\delta_{gm} = \sum_{i=1}^n f_i \delta_i; \text{ where } \sum_{i=1}^n f_i = 1 \quad (2)$$

where  $\delta_{gm}$  represents the geometric mean isotopic value,  $f_i$  represents the fraction, in each aliquot  $i$ , of total  $\text{CO}_2$  generated from the sample, and  $\delta_i$  represents the associated isotopic ratios.  $\Delta^{14}\text{C}_{gm}$  ( $-877 \pm 268\text{‰}$ , range:  $-996$  to  $0\text{‰}$ ) and  $\delta^{13}\text{C}_{gm}$  ( $-27.6 \pm 2.3\text{‰}$ , range:  $-28.8$  to  $-20.5\text{‰}$ ) characterize each whole sample subjected to RP (SI Table S2). Assuming sample composition to be a binary mixture of oil and background organic carbon (OC<sub>b</sub>), a Bayesian multisource isotope mixing model was employed to the radiocarbon data to estimate component fractions.<sup>61</sup> The mixing model has the same conventional formula as eq 3, but  $\delta_{gm}$  is replaced by  $\delta$  (the measured isotopic composition from a sample comprised of a mixture of endmembers). The model is able to incorporate known variability in endmembers and analytical error associated with the isotopic measurements. We use the most negative, blank-corrected  $\Delta^{14}\text{C}$  value measured for oil using RP AMS and the associated analytical uncertainty ( $-998.2 \pm 1.8\text{‰}$ ) for the oil endmember, and the mean  $\Delta^{14}\text{C}$  value and associated analytical uncertainty ( $86.9 \pm 4.0\text{‰}$ ) from RP AMS analysis of two unoiled marsh samples collected pre-DwH for the OC<sub>b</sub> endmember. Calculated fraction oil ( $f_{oil}$ ) values from radiocarbon data and the mixing model quantify oil in the  $\text{CO}_2$  aliquots (SI Table S2) and show high fractions of OC comprised of oil ( $0.899 \pm 0.216$ ). Applying to the mixing model geometric mean isotopic data calculated using eq 2 yields geometric mean fraction oil ( $f_{oil-gm}$ ) values that quantify oil for entire beach sediment, tar ball, and marsh samples ( $0.88 \pm 0.22$ ) analyzed by RP AMS.

The evolution of  $\text{CO}_2$  over the pyrolysis ramp estimates decomposition reaction rates ( $d[\text{reactants}]/dt$ ) for the mixture of compounds comprising the OC because temperature is linear with time.<sup>34,36</sup> RP data of  $\text{CO}_2$  concentration versus temperature are normalized to allow for comparison between samples with different amounts of carbon. As a result, the areas under reaction profiles are equal and can be interpreted by considering the percent of total OC that pyrolyzes within

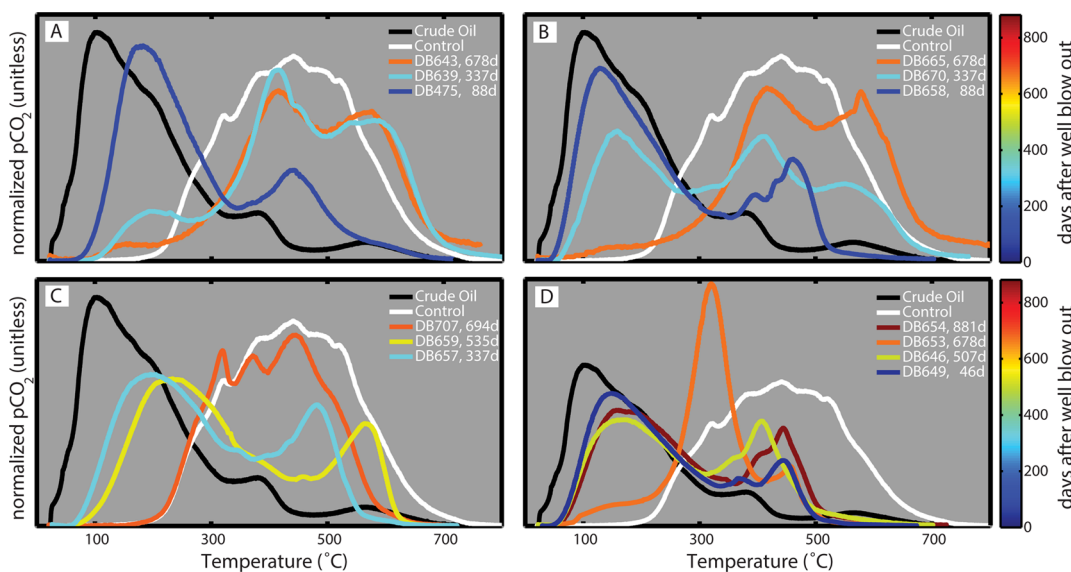


**Figure 3.** RP reaction profile trends over time for four sample types. Individual plots display evolution of  $\text{CO}_2$  over a smooth temperature ramp to 800 °C, and plots are colored based on time from the well blow-out. Profiles for Macondo crude oil (black) and a control sample from unoiled marsh (white) given for reference. A. Grand Isle beach sediments from the higher energy site. B. Grand Isle beach sediments from the lower energy site. C. Marsh samples from Bay Jimmy within Barataria Bay. D. Tar samples from Grand Isle.

certain temperature ranges. Pyrolysis at higher temperatures results from greater thermochemical stability. Here, we consider temperatures of <300 °C, 300–500 °C, and >500 °C as low, mid, and high, respectively.

Time series of RP data present varying thermochemical trends among the different sample types and environments (Figure 3). At 88 days, Grand Isle sediments from both high and low energy sites experience a majority of pyrolysis (63% and 68% of total pyrolysis, respectively) at low temperatures (<300 °C), but at 678 days these samples pyrolyze almost entirely (82 and 89%, respectively) at mid to high temperatures (>300 °C; Figure 3A and B). RP data for marsh samples from Bay Jimmy (Figure 3C) are characterized by significant (50%) low-temperature pyrolysis persisting through 535 days and minimal (16%) low-temperature pyrolysis at 694 days. Tar balls from Grand Isle (Figure 3D) continue to yield a majority of pyrolysis (59%) below 300 °C through 881 days, with the exception of a tar ball from 678 days that presents an anomalous reaction profile.

#### 4. DISCUSSION

**4.1. A Dominant Oil Signature in  $\Delta^{14}\text{C}$  and  $\delta^{13}\text{C}$  Data Through 881 Days.** Radiocarbon and stable carbon isotopic data for  $\text{CO}_2$  aliquots produced during RP demonstrate a dominance of oil-derived carbon in the sediments and soils for >678 days after the Macondo well explosion (Figure 2, SI Table S1). A large portion (88%) of  $\text{CO}_2$  aliquots were measured with radiocarbon values below  $-800\text{\textperthousand}$  (minimum of  $-998\text{\textperthousand}$ ) and correspondingly high calculated fraction oil values (maximum of 0.998; SI Table S2). For the tar balls, a maximum  $\Delta^{14}\text{C}$  value of  $-977\text{\textperthousand}$ , corresponding to a minimum  $f_{\text{oil}}$  value of 0.966 (SI Table S2), confirms compositions dominated by oil-derived C for 881 days, including the sample with an anomalous reaction profile (Figure 3D). Stable carbon isotopic data also support the prominence of oil in the OC of most  $\text{CO}_2$  aliquots. We use  $\delta^{13}\text{C}$  to indicate oil in pyrolysates but not for quantification purposes because  $\delta^{13}\text{C}$  is not as sensitive a tracer of oil as is  $\Delta^{14}\text{C}$  and because  $\Delta^{14}\text{C}$  inputs can be constrained by a binary

mixing model. The expected sources of carbon at the study sites and their associated  $\delta^{13}\text{C}$  values are oil ( $-27.3\text{\textperthousand}$ ), marine organic material ( $-20\text{\textperthousand}$ ), and brackish marsh organic material ( $-16.9$  to  $-12.5\text{\textperthousand}$ ).<sup>39,43,58,60,62</sup> Stable carbon isotopic data for the samples analyzed by RP indicate OC dominated by petrogenic carbon in all the samples, yielding a mean  $\delta^{13}\text{C}_{\text{gm}}$  value ( $-27.6 \pm 2.3\text{\textperthousand}$ ) comparable to that of the Macondo oil ( $-27.3\text{\textperthousand}$ ). RP  $\text{CO}_2$  aliquot  $\delta^{13}\text{C}$  data below the lowest expected endmember indicate that stable carbon isotopes are not uniform in the different compounds of the oil mixture and they are fractionated chemically and/or isotopically during RP, as previously observed.<sup>35,38,39</sup> Inclusion of  $\text{C}_3$  terrigenous carbon ( $\delta^{13}\text{C} = -34$  to  $-23\text{\textperthousand}$ )<sup>63</sup> is also possible and could account for  $\delta^{13}\text{C}$  values below that of oil. In the case of fractionation, this would not affect radiocarbon data as they are corrected for stable isotope values. No matter the reason, our results indicate that the process responsible for transformation of oil in these environments has not fractionated the oil-derived carbon isotopically.

**4.2. Evidence for Chemical Transformation of Oil and Derivatives.** Considering that isotopic data demonstrate the OC is dominated by oil for nearly all samples (Figure 2, SI Table S2), the observed changes in thermochemical stability (Figure 3) can be interpreted as evidence of oil stabilization through degradation. Therefore, we reject the null hypothesis that oil was removed from these depositional settings before undergoing transformation. Oil degradation is most apparent in the disappearance of low temperature pyrolysis over time, shifting the decomposition of the oil and derivatives to higher overall temperatures. This indicates an increase in thermochemical stability of the OC through time. In this study, oil transformation to more stable groups of compounds occurs fastest in higher energy beach sediments. Ramped pyrolysis data for sediments from the Grand Isle higher and lower energy sites (Figure 3A and B, respectively) display similar decreases in low-temperature pyrolysis and increase in high-temperature pyrolysis. Isotopic data for each reaction profile shows oil to be the major source of OC at all temperatures for both sites

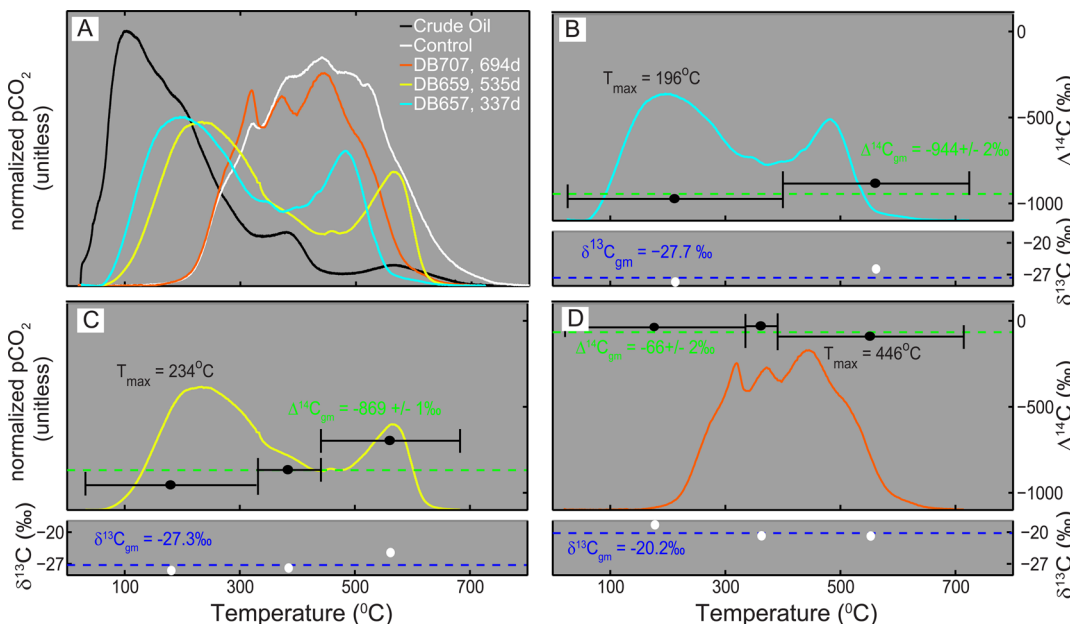


**Figure 4.** RP isotopic data for marsh samples. A. Trend in profiles over time. Profiles for Macondo crude oil (black) and a control sample from unoiled marsh (white) given for reference. B–D Profiles with isotopic data for samples at 337, 535, and 694 days. Left axis in top panel is  $\text{CO}_2$  evolution. Right axis is  $\Delta^{14}\text{C}$ . Horizontal bars indicate temperature intervals over which the aliquots of  $\text{CO}_2$  were collected. Bottom panel plots  $\delta^{13}\text{C}$  (points in white) for the same intervals.  $T_{\max}$  is temperature at which maximum pyrolysis occurs. Geometric mean isotopic values are shown by dashed lines in green ( $\Delta^{14}\text{C}$ ) and blue ( $\delta^{13}\text{C}$ ). Errors on the isotopic measurements are smaller than the symbols used to plot the values.

(Figure 2 and SI Figures S3 and S4). Evidence of faster oil degradation at the high energy site than at the low energy site exists at 337 d, with relatively more low temperature pyrolysis (42% of total pyrolysis) persisting at the lower energy site than at the high energy site (15%; Figure 3 A and B). Additionally, a lower  $\Delta^{14}\text{C}_{\text{gm}}$  value (by 103‰) and a correspondingly higher  $f_{\text{oil-gm}}$  value (by 0.095) for the low energy site at 337 days (SI Table S2) indicate a higher proportion of oil remaining there than at the high energy site due to a slower rate of oil degradation and/or dispersal. Similar RP profiles at 678 days (Figure 3A and B) indicate the oil at both sites had reached similar states of degradation by that point.

Marsh RP data (Figures 3C and 4) indicate slower oil transformation than in beach sediments. More low temperature pyrolysis in the marsh at 535 days (50%) than in the lower energy beach sediments at 337 days (42%) indicates greater preservation of less stable oil moieties in the marsh. A second peak shifted to higher temperatures between 337 and 535 days (Figure 3C) is likely due to a relative increase in  $\text{OC}_b$  (Figure 4 and SI Table S2). Pyrolysis at 694 days occurs fully in the temperature range of the control sample (Figures 3C and 4) and isotopic data confirm the lack of oil visible that day at Bay Jimmy (Figure 4 and SI Table S2). This sample indicates the importance of using both the reaction shape and the isotopic composition to discern transformation versus complete degradation or erosion of the oil contamination.

Transformation does not seem to occur within tar ball microenvironments, where only a crust of oil interacts with the surroundings and most oil mass is untouched (Figure 3D). Tar balls yielding a majority of pyrolysis (59%) at low temperatures through 881 days indicate preservation of the oil comprising the tar balls. A tar ball at 678 days ( $f_{\text{oil-gm}} = 0.998$ ) that upon collection resembled asphalt or black rubber presented a unique RP profile (Figure 3D) that we interpret as oil that has undergone a different degradative pathway than the other tar

balls. Aeppel et al.<sup>11</sup> determined that samples with a similar appearance collected at Grand Isle and the Chandeleur Islands, Louisiana, U.S.A., did not fit the two-dimensional gas chromatography flame ionization detection (GCxGC-FID) fingerprint of Macondo oil.

The relative oil transformation rates observed in our sample sets are in agreement with degradation rates in previous studies. Oil degradation was fastest at the high energy beach site because mechanical energy was greatest there and resulted in fastest dispersion and surface area maximization of oil in the water and sediments and greatest exchange between oil, pore- and overlying waters, microbes, oxygen, and nutrients.<sup>1,9,64,65</sup> Oil degradation was slower in the marsh than in the beach sediments due to less mechanical energy at the marsh. In addition, marshes contain high amounts of other organic material that can be preferentially consumed by microbial communities, thus limiting nutrients necessary for microbial consumption of oil.<sup>17,18</sup> Anoxia in marsh sediments can also slow oil degradation but is not considered to be a significant factor in this study because the marsh samples were collected from the surface. Tar balls degraded the most slowly because they protect the majority of their mass from exchange with water, sediments, microbes, oxygen, and nutrients by a small surface area-to-mass ratio.<sup>17,66</sup> Our findings are in agreement with other studies that have documented the persistence of tar balls.<sup>67,68</sup> Despite their heavily weathered appearance, tar balls shelter significant (~30%) concentrations of saturates, compounds that formed a relatively large portion (62–74%) of the Macondo crude oil.<sup>69</sup> Whereas Elango et al.<sup>68</sup> presents slow degradation of oil components in tar balls, our RP data present an even more extreme scenario: minimal degradation of labile oil compounds between 46 and 881 days after initiation of DwH. This evidence of such slow oil degradation in tar balls helps explain their persistence for years to decades in coastal environments after an oil spill.<sup>67</sup>

**4.3. Insight into Oil Transformation.** The stabilization of the oil-derived compounds observed in RP data likely result from both the loss of labile compounds and the conversion of labile compounds into more stable compounds (Figure 3, except 3D). Oil degradation has largely been considered in terms of the loss of certain compounds and has been evaluated through the use of ratios of GC-amenable compounds. The degradation product is more stable than the original oil because the more volatile and reactive compounds are preferentially lost and/or converted, leaving behind recalcitrant compounds (generally in the form of a growing unresolved complex mixture (UCM) in GC terminology). In the RP data from beach and marsh OC, we observe this in the loss of low temperature pyrolysis over time and the persistence of pyrolysis at mid and high temperatures (Figure 3). However, a question to be asked is whether the remaining compounds were present in the original oil or if some of them were generated during degradation. Recent efforts on DWH oil have provided new insight into the transformation of oil compounds. Two-dimensional gas chromatography (GC×GC) has helped show that degraded oil can be largely comprised of saturated hydrocarbons, present in the crude oil, as well as oxygenated hydrocarbons, such as carboxylic acids, that appear to be the result of biodegradation (carboxylic acids have been identified in biodegraded source oils for decades,<sup>70–73</sup> yet they had been largely ignored in oil contamination until recently<sup>11,69,74</sup>). The identification of stable compounds formed from crude oil components is significant because it demonstrates that degradation does not only imply the loss of compounds through evaporation or mineralization into CO<sub>2</sub>. In light of this information, we propose that the decrease in prominence of low-temperature pyrolysis and increase in the prominence of high-temperature pyrolysis presented here (Figure 3) is likely the result of both the loss of less thermochemically stable compounds and their conversion into more thermochemically stable compounds. Compounds that pyrolyze at mid- and high-temperatures are likely a combination of saturated hydrocarbons, oxygenated hydrocarbon residues, and other compounds yet to be identified in degraded oil.<sup>11,69,74,75</sup>

#### 4.4. Constraint of Specific Degradation Processes Using Ramped Pyrolysis Data.

Oil evaporated in the laboratory and tar from a rocky groin provide insight into the RP signatures of evaporation and biodegradation, the degradation processes that most affect oil in the environment.<sup>1,3,4,7,9,10</sup> The residue that remained after evaporating Macondo crude oil at 60 °C for 310 h shows a similar RP profile as the crude oil, but shifted to only slightly higher temperatures (61 °C according to  $T_{\max}$ , the temperature of maximum pyrolysis, Figure 5A). Thus, evaporation can account for the slight shift to higher temperatures of the prominent, low temperature peak in the reaction profiles of the 88 day beach sediments (Figure 3A and B). However, the evaporation of crude oil in the laboratory did not result in the nearly complete loss of low-temperature pyrolysis that occurred in beach sediment and marsh samples after 88 days. The RP profiles of two tar deposits collected from a rocky groin at Grand Isle (Figure 4B) exhibit a loss of low temperature pyrolysis similar to that observed in the sedimentary OC from Grand Isle and Bay Jimmy. One sample was taken from the top of the rocky groin where it was exposed to direct solar radiation and remained dry most of the time. These are conditions we deem less hospitable to microbes. The other sample was collected from within the rocky groin where it was out of direct sunlight

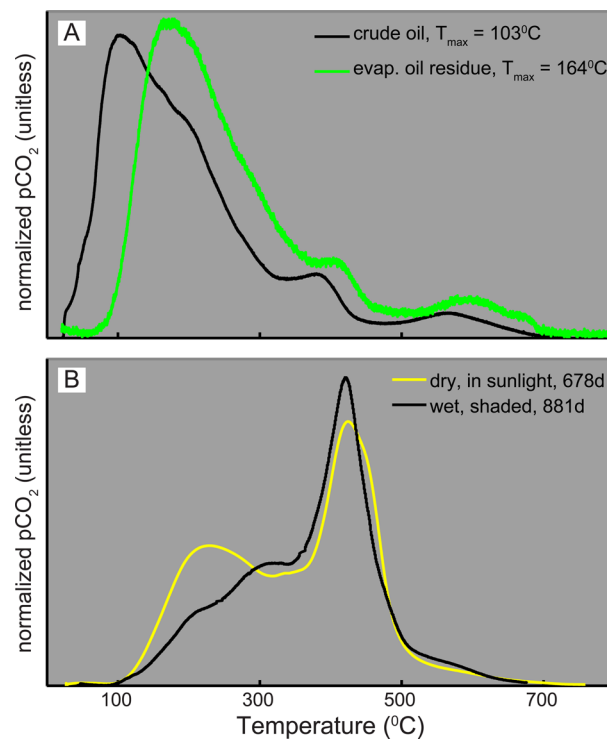


**Figure 5.** A. Oil evaporated at ~60 °C shows a loss of compounds below that temperature yet continues to present a dominant low temperature peak. B. Tar sampled from a rocky groin presents a loss of oil compounds that pyrolyze at low temperatures, similar to the oil in beach sediment and marsh samples.

and often wet from wave and tidal action; conditions more hospitable to microbes. The sample from the more hospitable environment displays a loss of low temperature pyrolysis relative to the sample from the inhospitable environment (Figure 5B). Isotopic data for both samples confirm their compositions to be largely oil ( $f_{oil-gm} = 0.986$  and 0.910). We interpret these two pairs of samples as evidence that the disappearance of low temperature pyrolysis observed in sedimentary beach and marsh OC over the course of 600+ days is largely due to biodegradation.

#### 4.5. Other Processes Affecting Isotopic Trends.

Isotopic data show evidence of stable isotope fractionation at the most depleted  $\Delta^{14}\text{C}$  values and mixing with other OC sources at less depleted  $\Delta^{14}\text{C}$  values. At 88 days, radiocarbon data pooled from the two barrier island sites (Figure 6A) show that oil is the only carbon source ( $\Delta^{14}\text{C} \approx -1000\text{\textperthousand}$ ), and there is no mixing occurring between sources of carbon. The variation in  $\delta^{13}\text{C}$  is interpreted as RP causing isotopic fractionation or chemical separation of oil components that are both isotopically ( $\delta^{13}\text{C}$ ) and thermochemically distinct. Stable carbon isotope fractionation has been observed before in RP,<sup>35,38,39</sup> however it is important to note that radiocarbon values, which are used to calculate  $f_{oil}$ , are corrected for stable carbon isotope composition<sup>34,40</sup> thus fractionation does not affect  $^{14}\text{C}$  quantification. As the oil mixes with OC<sub>b</sub> in the environment and  $\Delta^{14}\text{C}$  values become less negative (Figure 6A), a mixing relationship, with variation in both  $\delta^{13}\text{C}$  and  $\Delta^{14}\text{C}$ , dominates the fractionation signal. Increasing steepness of linearly regressed data in  $\delta^{13}\text{C}$ - $\Delta^{14}\text{C}$  space at different sampling dates (Figure 6A) indicates admixture of OC<sub>b</sub> over time. Data from tar samples show a similar trend but at a slower rate, indicating a slower rate of incorporation of OC<sub>b</sub> into tar

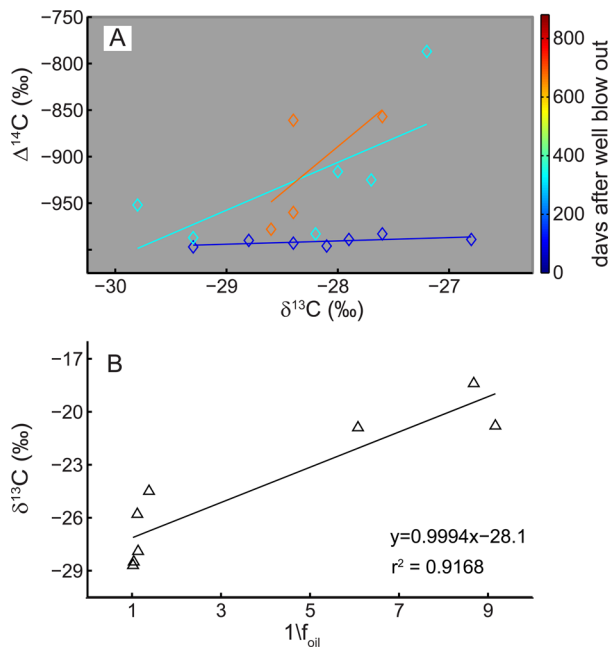


**Figure 6.** A. Carbon isotopic compositions of aliquots of sediment samples produced by RP AMS. Dark blue: 88 d; light blue: 337 d; orange: 678 d. Variation of the  $\delta^{13}\text{C}$  with minimal variation in  $\Delta^{14}\text{C}$  is interpreted as evidence of fractionation. Slopes of linear regressions for each date are interpreted to be proportional to degree of mixing (addition of OC<sub>b</sub> to the oil). B. Plotting  $\delta^{13}\text{C}$  vs  $1/f_{\text{oil}}$  for all CO<sub>2</sub> aliquots from marsh samples produces a Keeling-like plot that yields a  $\delta^{13}\text{C}$  estimate for oil of  $-27.1\text{‰}$  at  $1/f_{\text{oil}} = 1$ .

balls (SI Figure S6B). It is important to note that the amounts of OC<sub>b</sub> are small, but RP isotopic analysis is sensitive enough to reveal the isotopic effect. A mixing line that better encompasses this system's endmembers can be generated by linearly regressing all the marsh data together (Figure 6B) because earlier samples are comprised almost exclusively of oil and the marsh sample from 694 days is nearly devoid of oil. Plotting  $\delta^{13}\text{C}$  versus  $1/f_{\text{oil}}$  in a Keeling-like plot<sup>76</sup> (Figure 6B), as in Pendergraft et al.,<sup>39</sup> accurately estimates the  $\delta^{13}\text{C}$  value of Macondo oil ( $-27.1\text{‰}$  where  $1/f_{\text{oil}} = 1$ ) to within twice the measurement error ( $1\sigma = 0.1\text{‰}$ ) of the measured value ( $-27.3\text{‰}$ ).<sup>39,43</sup> Data at lower  $1/f_{\text{oil}}$  values (higher  $f_{\text{oil}}$ ) exhibit fractionation in their  $\delta^{13}\text{C}$  variation, whereas variation in both  $1/f_{\text{oil}}$  and  $\delta^{13}\text{C}$  at higher  $1/f_{\text{oil}}$  values (lower  $f_{\text{oil}}$ ) demonstrates admixture of OC<sub>b</sub>.

**4.6. Significance of Results.** Our RP isotope analysis of oil-impacted beach and marsh SOM presents transformation of oil by analyzing all of the OM in the system, including compounds not initially present in the petroleum contamination. For all three locations, higher shoreline energy implies faster dispersion of oil and greater exchange with water, sediments, microbes, oxygen, and nutrients.<sup>1,3,9,16–21</sup> Higher energy environments can also imply faster and more admixture with other ambient sources of organic material after the oil contamination event. Overall, isotopic data reveal that oil dominated the organic carbon in coastal Louisiana after the 2010 Deepwater Horizon oil spill and persisted, especially in tarballs, for 678–881+ days. Ramped pyrolysis reaction profiles show oil transformation in beach sediments and on the marsh surface and oil preservation in tar balls. These findings are in agreement with previous studies that found oil in tar balls, aggregates, and thick emulsions can persist in the environment

much longer than oil from the same source but in dispersed forms.<sup>17,18</sup> Relative oil degradation rates, from fastest to slowest for the four environments, are as follows: higher energy beach sediments > lower energy beach sediments > marsh surface > tar balls. Transformation of the oil seems to have been microbially mediated. Mixing processes are also recognized in isotope time series, particularly in the marsh, an environment rich in OC<sub>b</sub>. The persistence of oil in this region is important due to the vulnerability of the area where a large proportion of this oil was deposited. The presence of transformed oil compounds may prolong the effects of the oil deposition, especially in a sensitive and important ecosystem.

## ASSOCIATED CONTENT

### Supporting Information

Additional information as noted in the text. This material is available free of charge via the Internet at <http://pubs.acs.org>.

## AUTHOR INFORMATION

### Corresponding Author

\*E-mail: brosenheim@usf.edu.

### Present Address

<sup>†</sup>University of California at San Diego, Scripps Institution of Oceanography, La Jolla, California 92093 United States.

### Notes

The authors declare no competing financial interest.

## ACKNOWLEDGMENTS

The authors thank Dr. D. Finklestein (Hobart and William Smith Colleges) and Dr. A. Schimmelmann (Indiana University) for their assistance in field work and experimental design. We also thank all who assisted with sample collection and preparation. Analyses were funded by NSF grants EAR-1058517 and EAR-1045845 to BER and by the Consortium for Advanced Research on Transport of Hydrocarbon in the Environment (CARTHE). MAP was partially funded by Louisiana Sea Grant (NOAA) awarded to Dr. N. Gasparini and by CARTHE. Dr. C. Taylor (Tulane University) is acknowledged for providing a portion of her Macondo oil for this study. This manuscript benefitted from four anonymous reviews.

## REFERENCES

- Rashid, M. A. Degradation of Bunker C oil under different coastal environments of Chebaducto Bay, Nova Scotia. *Estuarine Coastal Mar. Sci.* **1974**, *2*, 137–144.
- Ward, D. M.; Atlas, R. M.; Boehm, P. D.; Calder, J. A. Microbial biodegradation and chemical evolution of oil from the Amoco spill. *Ambio* **1980**, *9* (6), 277–283.
- DeLaune, R. D.; Gambrell, R. P.; Pardue, J. H.; Patrick, W. H., Jr. Fate of petroleum hydrocarbons and toxic organics in Louisiana coastal environments. *Estuaries* **1990**, *13* (1), 72–80.
- Wolfe, D. A.; Hameedi, M. J.; Michel, J.; Payne, J. R.; Galt, J. A.; Watabayashi, G.; Braddock, J.; Hanna, S.; Short, J.; O’Claire, C.; Rice, S.; Sale, D. The fate of the oil spilled from the Exxon Valdez. *Environ. Sci. Technol.* **1994**, *28* (13), 561–568.
- Bence, A. E.; Kvenvolden, K. A.; Kennicutt, M. C. Organic geochemistry applied to environmental assessments of Prince William Sound, Alaska, after the Exxon Valdez oil spill—A review. *Org. Geochem.* **1996**, *24* (1), 7–42.
- Wang, Z.; Fingas, M.; Page, D. S. Review—Oil spill identification. *J. Chromatogr., A* **1999**, *843*, 369–411.
- Prince, R. C.; Garrett, R. M.; Bare, E. R.; Grossman, M. J.; Townsend, T.; Suflita, J. M.; Lee, K.; Owens, E. H.; Sergy, G. A.

- Braddock, J. F.; Lindstrom, J. E.; Lessard, R. R. The roles of photooxidation and biodegradation in long-term weathering of crude and heavy fuel oils. *Spill Sci. Technol. B* **2003**, *8* (2), 145–156, DOI: 10.1016/S1353-2561(03)00017-3.
- (8) Alaska North Slope Crude Blends; U.S. Department of Commerce; National Oceanic and Atmospheric Administration (NOAA); National Ocean Service; Office of Response and Restoration, Washington, DC, 2006. <http://response.restoration.noaa.gov/oil-and-chemical-spills/oil-spills/resources/alaska-north-slope-crude-blends.html>.
- (9) Owens, E. H.; Taylor, E.; Humphrey, B. The persistence and character of stranded oil on coarse-sediment beaches. *Mar. Pollut. Bull.* **2008**, *56*, 14–26, DOI: 10.1016/j.marpolbul.2007.08.020.
- (10) Atlas, R. M.; Hazen, T. C. Oil biodegradation and bioremediation: A tale of the two worst spills in U.S. history. *Environ. Sci. Technol.* **2011**, *45*, 6709–6715, DOI: 10.1021/es2013227.
- (11) Aepli, C.; Carmichael, C. A.; Nelson, R. K.; Lemkau, K. L.; Graham, W. M.; Redmond, M. C.; Valentine, D. L.; Reddy, C. M. Oil weathering after the Deepwater Horizon disaster led to the formation of oxygenated residues. *Environ. Sci. Technol.* **2012**, *46*, 8799–8807, DOI: 10.1021/es301538.
- (12) Liu, Z.; Liu, J.; Zhu, Q.; Wu, W. The weathering of oil after the Deepwater Horizon oil spill: Insights from the chemical composition of the oil from the sea surface, salt marshes and sediments. *Environ. Res. Lett.* **2012**, *7*, 035302 DOI: 10.1088/1748-9326/7/3/035302.
- (13) Ryerson, T. B.; Aikin, K. C.; Angevine, W. M.; Atlas, E. L.; Black, D. R.; Brock, C. A.; Fehsenfeld, F. C.; Gao, R.-S.; de Gouw, J. A.; Fahey, D. W.; Holloway, J. S.; Lack, D. A.; Lueb, R. A.; Meinardi, S.; Middlebrook, A. M.; Murphy, D. M.; Neuman, J. A.; Nowak, J. B.; Parrish, D. D.; Peischl, J.; Perring, A. E.; Pollack, I. B.; Ravishankara, A. R.; Roberts, J. M.; Schwarz, J. P.; Spackman, J. R.; Stark, H.; Warneke, C.; Watts, L. A. Atmospheric emissions from the Deepwater Horizon spill constrain air-water partitioning, hydrocarbon fate, and leak rate. *Geophys. Res. Lett.* **2011**, *38*, 1–6, DOI: 10.1029/2011GL046726.
- (14) Atlas, R. M. Effects of temperature and crude oil composition on petroleum biodegradation. *Appl. Microbiol.* **1975**, *30* (3), 396–403.
- (15) Hayes, M. O.; Michel, J.; Noe, D. C. Factors controlling initial deposition and long-term fate of spilled oil on gravel beaches. *International Oil Spill Conference Proceedings: March 1991*, **1991**, *1991*(1), 453–460. DOI: 10.7901/2169-3358-1991-1-453.
- (16) Gatellier, C. R.; Oudin, J. L.; Fusey, P.; Lacaze, J. C.; Priou, M. L. Experimental ecosystems to measure fate of oil spills dispersed by surface active products. *International Oil Spill Conference Proceedings: March 1973*. **1973**, *1973*(1), 497–504. DOI: 10.7901/2169-3358-1973-1-497.
- (17) Atlas, R. M. Microbial degradation of petroleum hydrocarbons: An environmental perspective. *Microbiol. Rev.* **1981**, *45* (1), 180–209.
- (18) Atlas, R. M. Petroleum biodegradation and oil spill bioremediation. *Mar. Pollut. Bull.* **1995**, *31* (4–12), 178–182.
- (19) McLachlan, A. Water filtration by dissipative beaches. *Limnol. Oceanogr.* **1989**, *34* (4), 774–780.
- (20) Forster, S.; Huettel, M.; Ziebis, W. Impact of boundary layer flow velocity on oxygen utilisation in coastal sediments. *Mar. Ecol.: Prog. Ser.* **1996**, *143*, 173–185.
- (21) Huettel, M.; Rusch, A. Transport and degradation of phytoplankton in permeable sediment. *Limnol. Oceanogr.* **2000**, *45* (3), 534–549.
- (22) Kingston, P. F. Long-term environmental impact of oil spills. *Spill Sci. Technol. B* **2002**, *7* (1–2), 53–61.
- (23) Reddy, C. M.; Eglington, T. I.; Hounshell, A.; White, H. K.; Xu, L.; Gaines, R. B.; Frysinger, G. S. The West Falmouth oil spill after thirty years: The persistence of petroleum hydrocarbons in marsh sediments. *Environ. Sci. Technol.* **2002**, *36*, 4754–4760, DOI: 10.1021/es020656n.
- (24) Peacock, E. E.; Nelson, R. K.; Solow, A. R.; Warren, J. D.; Baker, J. L.; Reddy, C. M. The West Falmouth oil spill: ~100 kg of oil found to persist decades later. *Environ. Forensics* **2005**, *6*, 273–281, DOI: 10.1080/15275920500194480.
- (25) White, H. K.; Liu, X.; Lima, A. L. C.; Eglington, T. I.; Reddy, C. Abundance, composition, and vertical transport of PAHs in marsh sediments. *Environ. Sci. Technol.* **2005**, *39*, 8273–8280, DOI: 10.1021/es050475w.
- (26) Crone, T. J.; Tolstoy, M. Magnitude of the 2010 Gulf of Mexico oil leak. *Science* **2010**, *330*, 634 DOI: 10.1126/science.1195840.
- (27) Barron, M. G. Ecological impacts of the Deepwater Horizon oil spill: Implications for immunotoxicity. *Toxicol. Pathol.* **2012**, *40*, 315–320, DOI: 10.1177/0192623311428474.
- (28) Silliman, B. R.; van de Koppel, J.; McCoy, M. W.; Diller, J.; Kasozi, G. N.; Earl, K.; Adams, P. N.; Zimmerman, A. R. Degradation and resilience in Louisiana salt marshes after the BP-Deepwater Horizon oil spill. *Proc. Natl. Acad. Sci. U. S. A.* **2012**, *109* (28), 11234–11239, DOI: 10.1073/pnas.1204922109.
- (29) Couvillion, B. R.; Barras, J. A.; Steyer, G. D.; Sleavin, W.; Fischer, M.; Beck, H.; Trahan, N.; Griffin, B.; Heckman, D. *Land Area Change in Coastal Louisiana from 1932 to 2010: U.S. Geological Survey Scientific Investigations Map 3164, Scale 1:265,000*, 2011.
- (30) Mendelsohn, I. A.; Andersen, G. L.; Baltz, D. M.; Caffey, R. H.; Carman, K. R.; Fleeger, J. W.; Joye, S. B.; Lin, Q.; Maltby, E.; Overton, E. B.; Rozas, L. P. Oil Impacts on coastal wetlands: Implications for the Mississippi River Delta ecosystem after the Deepwater Horizon oil spill. *BioScience* **2012**, *62* (6), 562–574, DOI: 10.1525/bio.2012.62.6.7.
- (31) Blum, M. D.; Roberts, H. H. Drowning of the Mississippi Delta due to insufficient sediment supply and global sea-level rise. *Nat. Geosci.* **2009**, *2*, 488–491, DOI: 10.1038/NGEO553.
- (32) Hester, M. W.; Mendelsohn, I. A. Long-term recovery of a Louisiana brackish marsh plant community from oil-spill impact: Vegetation response and mitigating effects of marsh surface elevation. *Mar. Environ. Res.* **2000**, *49*, 233–254.
- (33) McClenahan, G.; Turner, R. E.; Tweel, A. W. Effects of oil on the rate and trajectory of Louisiana marsh shoreline erosion. *Environ. Res. Lett.* **2013**, *8*, 044030 DOI: 10.1088/1748-9326/8/4/044030.
- (34) Rosenheim, B. E.; Day, M. B.; Domack, E. W.; Schrum, H.; Benthein, A.; Hayes, J. M. Antarctic sediment chronology by programmed-temperature pyrolysis: Methodology and data treatment. *Geochem. Geophys. Geosyst.* **2008**, *9* (4), Q04005 DOI: 10.1029/2007GC001816.
- (35) Rosenheim, B. E.; Galy, V. Direct measurement of riverine particulate organic carbon age structure. *Geophys. Res. Lett.* **2012**, *39*, L19703 DOI: 10.1029/2012GL052883.
- (36) Rosenheim, B. E.; Roe, K. M.; Roberts, B. J.; Kolker, A. S.; Allison, M. A.; Johannesson, K. H. River discharge influences on particulate organic carbon age structure in the Mississippi/Atchafalaya River system. *Global Biogeochem. Cycles* **2013a**, *27*, 1–13, DOI: 10.1002/gbc.20018.
- (37) Rosenheim, B. E.; Santoro, J. A.; Gunter, M.; Domack, E. W. Improving Antarctic sediment  $^{14}\text{C}$  dating using ramped pyrolysis: An example from the Hugo Island Trough. *Radiocarbon* **2013b**, *55* (1), 115–126, DOI: 10.2458/azu\_js\_rc.v55i1.16234.
- (38) Rosenheim, B. E.; Pendergraft, M. A.; Flowers, G. C.; Carney, R.; Sericano, J.; Amer, R. M.; Chanton, J.; Dincer, Z.; Wade, T. Employing extant stable carbon isotope data in Gulf of Mexico sedimentary organic matter for oil spill studies. *Deep Sea Res., Part II* **2014**, DOI: 10.1016/j.dsr2.2014.03.020.
- (39) Pendergraft, M. A.; Dincer, Z.; Sericano, J. L.; Wade, T.; Kolasinski, J.; Rosenheim, B. E. Linking ramped pyrolysis isotope data to oil content through PAH analysis. *Environ. Res. Lett.* **2013**, *8*, 044038 DOI: 10.1088/1748-9326/8/4/044038.
- (40) Stuiver, M.; Pollach, H. A. Reporting of  $^{14}\text{C}$  data. *Radiocarbon* **1977**, *19* (3), 355–363.
- (41) White, H. K.; Reddy, C. M.; Eglington, T. I. Radiocarbon-based assessment of fossil fuel-derived contaminant associations in sediments. *Environ. Sci. Technol.* **2008**, *42*, 5428–5434, DOI: 10.1021/es000478x.
- (42) Ahad, J. M. E.; Burns, L.; Mancini, S.; Slater, G. F. Assessing microbial uptake of petroleum hydrocarbons in groundwater systems

- using natural abundance radiocarbon. *Environ. Sci. Technol.* **2010**, *44*, 5092–5097, DOI: 10.1021/es100080c.
- (43) Graham, W. M.; Condon, R. H.; Carmichael, R. H.; D'Ambra, I.; Patterson, H. K.; Linn, L. J.; Hernandez, F. J., Jr. Oil carbon entered the coastal planktonic food web during the Deepwater Horizon oil spill. *Environ. Res. Lett.* **2010**, *5*, 045301 DOI: 10.1088/1748-9326/5/4/045301.
- (44) Chanton, J. P.; Cherrier, J.; Wilson, R. M.; Sarkodee-Ado, J.; Bosman, S.; Mickle, A.; Graham, W. M. Radiocarbon evidence that carbon from the Deepwater Horizon spill entered the planktonic food web of the Gulf of Mexico. *Environ. Res. Lett.* **2012**, *7*, 045303 DOI: 10.1088/1748-9326/7/4/045303.
- (45) Cherrier, J.; Sarkodee-Ado, J.; Guilderson, T. P.; Chanton, J. P. Fossil carbon in particulate organic matter in the Gulf of Mexico following the Deepwater Horizon event. *Environ. Res. Lett.* **2014**, *1* (1), 108–112.
- (46) Mahmoudi, N.; Fulthorpe, R. R.; Burns, L.; Mancini, S.; Slater, G. F. Assessing microbial carbon sources and potential PAH degradation using natural abundance  $^{14}\text{C}$  analysis. *Environ. Pollut.* **2013**, *175*, 125–130, DOI: 10.1016/j.envpol.2012.12.020.
- (47) Silverman, S. R.; Epstein, S. Carbon isotopic compositions of petroleum and other sedimentary organic materials. *Am. Assoc. Pet. Geol. Bull.* **1958**, *42* (5), 998–1012.
- (48) Matthews, D. E.; Hayes, J. M. Isotope-ratio-monitoring gas chromatography-mass spectrometry. *Anal. Chem.* **1978**, *50* (11), 1468–1473.
- (49) Chung, H. M.; Brand, S. W.; Grizzel, P. L. Carbon isotope geochemistry of Paleozoic oils from Big Horn Basin. *Geochim. Cosmochim. Acta* **1981**, *45*, 1803–1815.
- (50) Macko, S. A.; Parker, P. L.; Botello, A. V. Persistence of spilled oil in a Texas salt marsh. *Environ. Pollut. B* **1981**, *2*, 119–128.
- (51) Macko, S. A.; Parker, P. L. Stable nitrogen and carbon isotope ratios of beach tars on South Texas barrier islands. *Mar Environ. Res.* **1983**, *10*, 93–103.
- (52) Sofer, Z. Stable carbon isotope compositions of crude oils: Application to source depositional environments and petroleum alteration. *AAPG Bull.* **1984**, *68* (1), 31–49.
- (53) Mansuy, L.; Philp, R. P.; Allen, J. Source identification of oil spills based on the isotopic composition of individual components in weathered oil samples. *Environ. Sci. Technol.* **1997**, *31*, 3417–3425.
- (54) Wang, Z.; Fingas, M.; Landriault, M.; Sigouin, L. Identification and linkage of tarballs from the coasts of Vancouver Island and Northern California using GC/MS and isotopic techniques. *J. High Resolut. Chromatogr.* **1998**, *21* (7), 383–395.
- (55) Pond, K. L.; Huang, Y.; Wang, Y.; Kulpa, C. F. Hydrogen isotopic composition of individual n-alkanes as an intrinsic tracer for bioremediation and source identification of petroleum contamination. *Environ. Sci. Technol.* **2002**, *36*, 724–728.
- (56) Li, Y.; Xiong, Y.; Yang, W.; Xie, Y.; Li, S.; Sun, Y. Compound-specific stable carbon isotopic composition of petroleum hydrocarbons as a tool for tracing the source of oil spills. *Mar. Pollut. Bull.* **2009**, *58*, 114–117.
- (57) Natter, M.; Keevan, J.; Wang, Y.; Keimowitz, A. R.; Okeke, B. C.; Son, A.; Lee, M. Level and degradation of Deepwater Horizon spilled oil in coastal marsh sediments and pore-water. *Environ. Sci. Technol.* **2012**, *46*, 5744–5755, DOI: 10.1021/es300058w.
- (58) Chmura, G. L.; Aharon, P.; Socki, R. A.; Abernethy, R. An inventory of  $^{13}\text{C}$  abundances in coastal wetlands of Louisiana, USA: Vegetation and sediments. *Oecologia* **1987**, *74*, 264–271.
- (59) Brodie, C. R. Evidence for bias in C/N,  $\delta^{13}\text{C}$  and  $\delta^{15}\text{N}$  values of aquatic and terrestrial organic materials due to acid pre-treatment methods. *Pages News* **2011**, *19* (2), 65–67.
- (60) Sharp, Z. *Principles of Stable Isotope Geochemistry*; Prentice Hall: Upper Saddle River, NJ, 2007.
- (61) Parnell, A. C.; Inger, R.; Bearhop, S.; Jackson, A. L. Source partitioning using stable isotopes: Coping with too much variation. *PLoS One* **2010**, *5*, e9672 DOI: 10.1371/journal.pone.0009672.
- (62) Haines, E. B. Stable carbon isotope ratios in the biota, soils and tidal water of a Georgia salt marsh. *Estuarine Coastal Mar. Sci.* **1976**, *4*, 609–616.
- (63) Smith, B. N.; Epstein, S. Two categories of  $^{13}\text{C}/^{12}\text{C}$  ratios for higher plants. *Plant Physiol.* **1971**, *47*, 380–384.
- (64) Burns, K. A.; Garrity, S. D.; Jorissen, D.; MacPherson, J.; Stoelting, M.; Tierney, J.; Yelle-Simmons, L. The Galeta oil spill. II. Unexpected persistence of oil trapped in mangrove sediments. *Estuarine Coastal Shelf Sci.* **1994**, *38*, 349–364.
- (65) Mortazavi, B.; Horel, A.; Beazley, M. J.; Sobecky, P. A. Intrinsic rates of hydrocarbon biodegradation in Gulf of Mexico intertidal sandy sediments and its enhancement by organic substrates. *J. Hazard. Mater.* **2013**, *244–245*, 537–544, DOI: 10.1016/j.jhazmat.2012.10.038.
- (66) Short, J. W.; Irvine, G. V.; Mann, D. H.; Maselko, J. M.; Pella, J. J.; Lindeberg, M. R.; Payne, J. R.; Driskell, W. B.; Rice, S. D. Slightly weathered Exxon Valdez oil persists in Gulf of Alaska beach sediments after 16 years. *Environ. Sci. Technol.* **2007**, *41*, 1245–1250, DOI: 10.1021/es0620033.
- (67) Kvenvolden, K. A.; Hostettler, F. D.; Carlson, P. R.; Rapp, J. B.; Threlkeld, C. N.; Warden, A. Ubiquitous tar balls with a California-source signature on the shorelines of Prince William Sound, Alaska. *Environ. Sci. Technol.* **1995**, *29*, 2684–2694.
- (68) Elango, V.; Urbano, M.; Lemelle, K. R.; Pardue, J. H. Biodegradation of MC252 oil in oil:sand aggregates in a coastal headland beach environment. *Front. Microbiol.* **2014**, *5*, 161 DOI: 10.3389/fmicb.2014.00161.
- (69) Gros, J.; Reddy, C. M.; Aepli, C.; Nelson, R. K.; Carmichael, C. A.; Arey, J. S. Resolving biodegradation patterns of persistent saturated hydrocarbons in weathered oil samples from the Deepwater Horizon disaster. *Environ. Sci. Technol.* **2014**, *48* (3), 1628–1637, DOI: 10.1021/es4042836.
- (70) Behar, F. H.; Albrecht, P. Correlations between carboxylic acids and hydrocarbons in several crude oils. Alteration by biodegradation. *Org. Geochem.* **1984**, *6*, 597–604.
- (71) Jaffe, R.; Gallardo, M. T. Application of carboxylic acid biomarkers as indicators of biodegradation and migration of crude oils from the Maracaibo Basin, western Venezuela. *Org. Geochem.* **1993**, *20* (7), 973–984.
- (72) Meredith, W.; Kelland, S.-J.; Jones, D. M. Influence of biodegradation on crude oil acidity and carboxylic acid decomposition. *Org. Geochem.* **2000**, *31*, 1059–1073.
- (73) Watson, J. S.; Jones, D. M.; Swannell, R. P. J.; van Duin, A. C. T. Formation of carboxylic acids during aerobic biodegradation of crude oil and evidence of microbial oxidation of hopanes. *Org. Geochem.* **2002**, *33*, 1153–1169.
- (74) Hall, G. J.; Frysinger, G. S.; Aepli, C.; Carmichael, C. A.; Gros, J.; Lemkau, K. L.; Nelson, R. K.; Reddy, C. M. Oxygenated products of Deepwater Horizon oil come from surprising precursors. *Mar. Pollut. Bull.* **2013**, *75*, 140–149, DOI: 10.1016/j.marpolbul.2013.07.048.
- (75) Lemkau, K. L.; McKenna, A. M.; Podgorski, D. C.; Rodgers, R. P.; Reddy, C. M. Molecular evidence of heavy-oil weathering following the M/V Cosco Busan spill: Insights from Fourier transform ion cyclotron resonance mass spectrometry. *Environ. Sci. Technol.* **2014**, *48*, 3760–3767, DOI: 10.1021/es403787u.
- (76) Keeling, C. D. The concentration and isotopic abundances of atmospheric carbon dioxide in rural areas. *Geochim. Cosmochim. Acta* **1958**, *13*, 322–334.

## ■ NOTE ADDED AFTER ASAP PUBLICATION

This article published August 22, 2014 with errors throughout the paper. The corrected version published August 27, 2014.